Advances in Weed Science formerly Planta Daninha

SPECIAL TOPICS

Experimental methods and emerging technologies in weed science

RESEARCH ARTICLE

Protoporphyrinogen oxidase inhibitors discovered by Artificial Intelligence platform

Abigail L. Barker[a], Yosef Geva[b], Eyal Simonovsky[b], Netta Shemesh[b], Yael Phillip[b], Ifat Shub[b], Franck E. Dayan[a]*

[a] Department of Agricultural Biology, Colorado State University, Fort Collins CO USA. [b] Agrematch Ltd., Plaut 10 St., Rehovot Science Park, Israel.

Abstract: **Background:** Weed control is essential in modern agriculture, though it has become more difficult with the emergence of resistance to most current herbicides and the slow registration process for new compounds.

Objective: Identify herbicide candidates using an innovative artificial intelligence algorithm that takes into effect biological parameters with the goal of reducing research and development time of new herbicides.

Results: We describe the discovery of 4-chloro-2-pentenamides as novel inhibitors of protoporphyrinogen oxidase (PPO), a known herbicide target site, by the Agrematch AI. Their herbicidal activity was evaluated in greenhouse assays, with the highest performing compound (AGR001) showing good activity pre-emergent at 150 g ha^{-1} and post emergent at 50 g ha^{-1} on the troublesome weed Palmer amaranth (*Amaranthus palmeri*). A lack of activity is reported on PPO resistant Palmer amaranth carrying the glycine 210 deletion (ΔG210) mutation.

Conclusions: The mode of action of 4-chloro-2-pentenamides was confirmed by the herbicide-dependent accumulation of protoporphyrin IX, subsequent light-dependent loss of membrane integrity, and direct *in vitro* inhibition of PPO. Modeling of these inhibitors' docking in the active site of PPO shows that their flexible side chains can accommodate several binding poses in the catalytic domain.

Keywords: protoporphyrinogen oxidase; novel herbicides; 4-chloro-2-pentenamides; artificial intelligence

Journal Information:
ISSN - 2675-9462
Website: http://awsjournal.org
Journal of the Brazilian Weed Science Society

How to cite: Barker AL, Geva Y, Simonovsky W, Shemesh N, Phillip Y, Shub I, Dayan FE. Protoporphyrinogen oxidase inhibitors discovered by Artificial Intelligence platform. Adv Weed Sci. 2023;41:e020230025.
https://doi.org/10.51694/AdvWeedSci/2023;41:00011

Approved by:
Editor in Chief: Carol Ann Mallory-Smith
Associate Editor: Hudson Kagueyama Takano

Conflict of Interest: The authors declare that there is no conflict of interest regarding the publication of this manuscript.

Received: May 15, 2023
Approved: August 3, 2023

* Corresponding author:
<franck.dayan@colostate.edu>

1. Introduction

Current agriculture faces new struggles against unpredictable weather pattern changes associated with climate change and managing a myriad of pests that impact crop productivity. Weeds are the most problematic pests because these undesirable plants reduce crop yields by competing for space and resources (light, nutrients, water) and cause billions of dollars in annual loss (Pimentel et al., 2005; Soltani et al., 2016). Consequently, modern agricultural practices rely heavily on the use of synthetic herbicides. While herbicides have been a major contributor to the success of agriculture, they have imposed a strong selection pressure over millions of farming acres, leading to the evolution of herbicide resistance in hundreds of weed species (Heap, 2023). Both target-site resistance (TSR) and non-target-site resistance (NTSR) mechanisms have evolved to most herbicide classes (Gaines et al., 2020).

Nearly three decades without new herbicide modes of action (MoA) have left farmers in need of new, effective tools. New weed management methods are being developed to address the current weed resistance problems, including non-chemical approaches (Fennimore, Cutulle, 2019; Westwood et al., 2018), but chemical tools remain the most cost effective and no-tillage friendly (Cooper, Dobson, 2007). Recently, there has been a flurry of reports of new modes of action (Dayan, 2019). Most of these reports are from research groups within the Agrochemical industry. However, several startup companies have joined this effort with novel approaches to the discovery of interesting chemistries and new modes of action.

Understanding the process by which companies discover new herbicides grants insight into the lack of new herbicide options. There are five main steps to the development of a crop protection agent, which take on average 11 years of early research (Peters, Strek, 2018): 1) discovery, when a molecule is identified through some pipeline and its MoA and toxicity are investigated; 2) optimization, when the molecule is taken through formulation improvements and greenhouse testing against crops and weeds; 3) field trials, when this testing is taken to realistic conditions and large-scale safety studies; 4) development, which includes regulatory hurdles and registration of the commercial product; and 5) launch, when the product is released and stewarded by the company. Due to tightening registration regulations and the requirement for molecules with low toxicity, companies are screening upwards of 160,000 molecules to find one lead compound (Peters, Strek, 2018). Large agrochemical companies differ from startup companies (e.g., Agrematch,

MoA Technology and Enko) by relying mostly on large scale, automated screening processes utilizing available molecule libraries. On the other hand, startup companies have developed innovative approaches to screen extremely large numbers of compounds and methods to guide them to new MoA.

Agrematch is a unique data-science product discovery and development company catering to industries that require novel compounds for their products, initially focused on agriculture and food industries. Agrematch utilizes compound-based data analytics to predict early and downstream considerations which are necessary for successful product launch.

Agresense, the Agrematch artificial intelligence (AI) algorithm system has been developed for rational identification of molecules with desired compound-organism interaction. This multi-layered system utilizes advanced AI and machine learning (ML)/Deep Learning (DL) algorithms and other data science concepts combined with biology, chemistry, and agriculture knowledge to provide insights that help make informed decisions along the product development journey (Muller et al., 2022; von Lilienfeld, Burke, 2020). The Agresense model generation platform accesses a database of ~1.2B compounds with relevant training positive and negative datasets. In most cases, it takes multiple training iterations that sometimes require new data generation to create a robust predictive module. Once trained, the predictive module can be used for the desired application where every use contributes to the accuracy of the prediction. Each model has different characteristics which depend on the complexity of the question and the domain it searches; each model run may take from milliseconds with a single computer to days with thousands of cloud-activated CPUs. The iterative process includes testing the compounds identified by Agresense for their herbicidal activity in the lab and feeding the results back into the Agresense system to optimize it. Additional iterations of compound libraries are created until its MoA classifier algorithm predicts whether these compounds have a new MoA or belong to an existing HRAC class (Figure 1). A key use case of Agresense is the discovery and characterization of bioactive compounds, such as crop protection and crop enhancement products by screening the vast chemical universe for compounds with the desired functionality.

We report in this paper a chemical class of herbicide discovered using the AI algorithm developed by Agrematch. These molecules were predicted to target protoporphyrinogen oxidase (PPO). PPO is a key enzyme in porphyrin biosynthesis (Dayan, Duke, 2010) and herbicides with this MoA (Group 14) induce rapid death of the foliage due to the accumulation of a photodynamic metabolic intermediate. *In vivo* and *in vitro* experiments confirmed that these 4-chloro-2-pentenamides are PPO inhibitors.

2. Material and Methods

2.1 Plant material and growth

For herbicidal activity assays, Palmer amaranth (*Amaranthus palmeri* S. Watson), rough cocklebur (*Xanthium strumarium* L.), chinese thorn-apple (*Datura quercifolia* Kunth), black nightshade (*Solanum nigrum* L.) and mat amaranth (*Amaranthus blitoides* S. Watson) were seeded in pots with a potting mix (Peat Moss and vermiculite, Zohar 42, Tuff Substrates, Israel) and grown in either growth-chamber or net-house. Growth chamber conditions were 16 h light/8 h dark cycles with 30°C/25°C cycles respectively. Light intensity was 700 $\mu mol \cdot m^{-2} \cdot s^{-1}$. Net-house conditions were approximately 12 h light/12 h dark cycles with 26 °C on average. All plants were watered as needed.

Cucumber seedlings (cultivar Straight eight) were planted in trays with Pro-Mix (Premier Tech Horticulture) and grown in the greenhouse for up to 3 weeks to collect fresh cotyledons. These plants were discarded once the

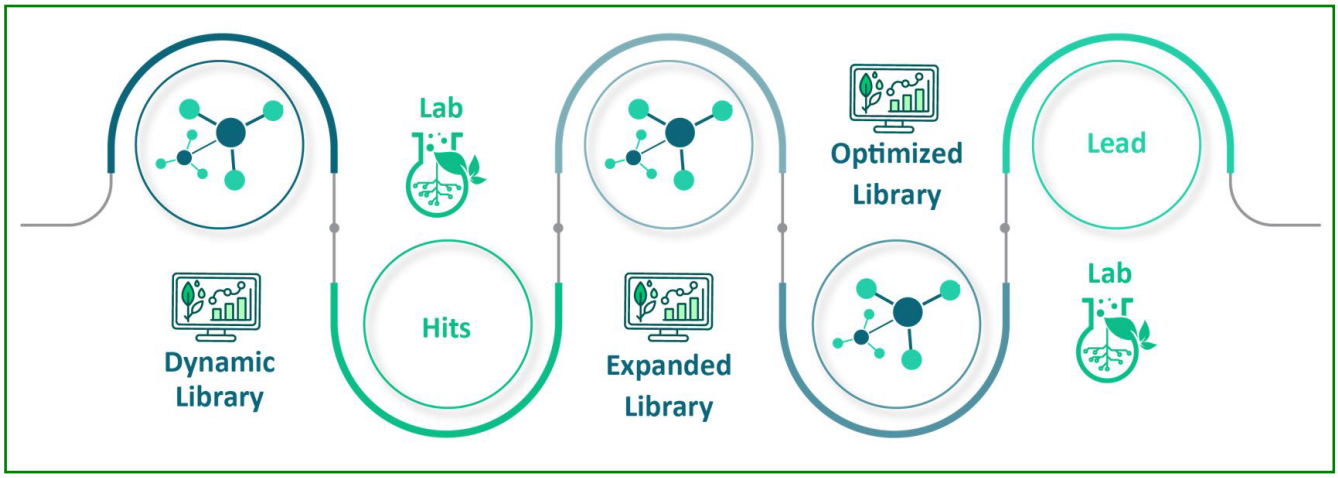

Figure 1 - An illustration of Agrematch platform iterative process, of in-silico screening, laboratory validation and feedback to the computational system to generate advanced functional compounds libraries.

2nd true-leaf started to emerge. Palmer amaranth plants that were either sensitive (S) or resistant (R) to PPO inhibitors due to a glycine210 deletion (Dayan et al., 2010; Patzoldt et al., 2006; Salas-Perez et al., 2018) were grown in the greenhouse for 4 weeks under similar conditions. All plants were watered as needed.

2.2 Herbicidal activity

For pre-emergence growth-chamber assays, compounds were dissolved in DMSO and diluted in water to a final concentration of 10-100 mg L^{-1} with 2% DMSO. Seeds were sown in pots containing wet potting mix to a depth of about 1 cm, covered, and immediately sprayed using a VL-SET Paasche Airbrush at a 3,000 L ha^{-1} application volume. Pots were watered 24 hr after application.

For post-emergence growth-chamber assays, compounds were dissolved in DMSO and diluted in water to a final concentration of 25-250 mg L^{-1} with 2% DMSO. Break-Thru® S-240 (EVONIK) at a final concentration of 0.05% was added. Compounds were sprayed using a VL-SET Paasche Airbrush at a 1,000 L ha^{-1} application volume (https://www.paascheairbrush.com/VL-3AS). Weeds were sprayed at the 4-6 leaf stage (8 d after sowing).

For post-emergence net-house assays, 300 mg L^{-1} of compound AGR001 was dissolved with 900 mg L^{-1} xylenes, 73 mg L^{-1} ethoxylated castor oil (Kolliphor® RH 40) and 48 mg L^{-1} calcium dodecylbenzene sulfonate (Rhodacal® 60be) in water. Break-Thru® S-240 (EVONIK) at a final concentration of 0.05% was added. Weeds were sprayed using a VL-SET Paasche Airbrush at a 1,000 L ha^{-1} application volume at the 4-6 leaf stage (2-leaf stage for *D. ferox*). All pre- and post-emergence assays were performed with three replicates per treatment and repeated at least 3 times.

Herbicidal activity was assessed and scored 7 days after application by visual inspection of the weeds in comparison to untreated controls. Activity score was in the range of 0 to 100, where 0 represents no herbicidal activity and 100 represents the maximal herbicidal activity (i.e., total death of the weed).

2.3 Electrolyte leakage

First, time-course experiments were conducted over 40 h to measure the effect of AGR001 or AGR002 on electrolyte leakage from cucumber cotyledons using a modified method of Dayan and Watson (2011). For each compound, 36 discs (6 mm diam.) were cut from 7- to 15-day-old cucumber cotyledons and placed in a petri dish. The discs were floated over 5 mL of MES buffer (pH 6.5) with 2% sucrose with 100 µg mL^{-1} of either AGR001 or AGR002. This was conducted in low light intensity to prevent photodynamic damage (less than 150 µmol m^{-2} s^{-1}).

Once the plates were prepared, the initial conductivity (a measure of electrolyte leakage) was measured using a FiveEasy Plus FP30 conductivity meter connected to an InLab 751-4 mm microprobe (Mettler Toledo, Columbus, OH 43240). The plates were kept in the dark at room temperature for 16 h. Conductivity was measured after the dark incubation period and then the plates were moved into an LED-30L1 LED high intensity growth chamber (Percival, Perry Iowa 50220). Conductivity was measured 1, 5, 10, 24 h after exposure to light intensity (approx. 1,050 µmol m^{-2} s^{-1}).

Dose-response curve experiments were conducted with AGR001 and AGR002 at 1, 3, 10, 30, 100 and 300 µM. The control treatment consisted of DMSO alone to determine the relative potency of these molecules. Conductivity was measured as described above after 16 h dark incubation followed by 24 h exposure to high light intensity.

The effect of AGR001 and AGR002 was tested on biotypes of S and R Palmer amaranth plants. For this experiment, 60 leaf discs from 4-week-old Palmer amaranth were used. Concentrations used were 10 µM AGR001 and 100 µM AGR002, conductivity was compared to controls with DMSO alone.

2.4 Protoporphyrin IX accumulation

The effects of AGR001 and AGR002 on protoporphyrin IX (proto) levels were measured in cucumber cotyledons exposed to 300 µM of either compound and compared to DMSO control after 16 h dark incubation. Proto extraction and analysis followed a protocol described by Dayan et al. (2015). Approximately 0.2 g of cotyledonary tissue was ground to a powder in liquid nitrogen and homogenized in 2 mL of extraction solvent (methanol:0.1 M NH_4OH, 9:1) and centrifuged at 10,000 × g for 15 min. The supernatant was saved and the pellet rehomogenized in 1 mL of extraction solvent, centrifuged again at 10,000 × g for 15 min. Supernatants were pooled and then filtered through a 0.2-µm nylon syringe membrane filter before quantification with the LC-MS/MS system. Proto was separated in a biphenyl column (100 by 4.6 mm, 2.6 µm, 40 °C) at a flow rate of 0.4 mL min^{-1} using a linear gradient of methanol (B) and 10 mM ammonium acetate (A): 0 min, 50% B; 8min, 70% B; 11 min, 90% B; 13 min, 90% B; 13.5 min, 50% B; 17 min, 50% B. The MRM was optimized to 340.10 > 227.95 (Moulin, Smith, 2008). A standard curve generated with serial dilutions of technical grade protoporphyrin IX (MilliporeSigma, St. Louis, MO) was used for quantification. Limit of detection (LOD) and limit of quantification (LOQ) for proto were 0.05 ng $µL^{-1}$ and 0.15 ng $µL^{-1}$.

2.5 Protoporphyrinogen oxidase activity

PPO was obtained by expression and purification of the *Amaranthus tuberculatus* wild type isoform as described by Dayan et al. (2010). Briefly, the cell line was cultured overnight at 37 °C in 250 mL of LB with ampicillin, which

was diluted into 1 L of LB with antibiotic and grown for 1 h before induction with 1 mM IPTG. After induction, the culture was grown at 25 °C for 5 h. Cells were harvested by centrifugation at 2,000 × g and washed with 0.1% NaCl. Cells were lysed by sonication (Model 120 Sonic Dismembrator with a Model CL-18 1/8 inch probe, Thermo Fisher Scientific, Waltham, MA, USA) in 3 × 30 s bursts with 60 s on ice in between in 50 mM sodium phosphate pH 7.5, 500 mM NaCl, 5 mM imidazole, 5% glycerol and 1 µg mL^{-1} leupeptin. After lysis 1 unit of benzonase (Millipore Sigma, Burlington, MA, USA) and 1 mM PMSF were added. Debris were removed by centrifugation for 30 min at 2,000 × g. Proteins were purified on a HisPur Ni-NTA Spin Column (Thermo Fisher Scientific, Waltham, MA, USA) as per the instructions with elution at 20 mM sodium phosphate, 300 mM sodium chloride 250 mM imidazole, pH 7.4. Protein was desalted on a PD-10 column (GE Healthcare Bio-Sciences Corp., Piscataway, NJ, USA) equilibrated with 20 mM sodium phosphate, pH 7.5, 5 mM $MgCl_2$, 1 mM EDTA and 17% glycerol. Pure PPO which was stored at -80 °C until use.

Protoporphyrinogen was prepared by reducing proto with sodium amalgam as described by Jacobs and Jacobs (1982). Assays were conducted with 20 µg of protein per replicate as described by Dayan et al. (2010) with specific modifications for our spectrophotometer as follows: enzymatic activity was measured on a spectrofluorometer (Synergy H1, Agilent Technologies, Wilmington, DE USA). Excitation and emission wavelengths were set to 395 and 633 nm, respectively. The assay was carried out in black microplates (Costar 3915) under kinetics condition over 10 min. Enzyme activity was measured based on the linear portion of the curve. Proto amounts were calculated based on a calibration curve of proto standard (Sigma-Aldrich, Inc., St. Louis, MO 68178) at concentrations ranging from 8 nM to 2 µM (Supplemental Figure 1). AGR001 and AGR002 were tested at concentrations ranging from 0.3 to 333 µM and compared to untreated control that received the same volume of solvent. Statistical analysis was performed using the R software (v 4.1.0). Dose responses were fit using the DRC package (Ritz et al., 2015). Regression curves were imported into Prism 9.1.1 (GraphPad, San Diego, CA 92103).

2.6 Docking study

All herbicide structures were downloaded as 3-D.sdf files from PubChem (Kim et al., 2021). The two experimental compounds were built using a molecular modelling and computational chemistry application (Spartan18, Wavefunction, Inc. Irvine, CA 92612). The bond angles and length were corrected, and the atom energies were calculated by submitting all the molecules to geometric minimization using density function theory calculations (wB97X-D 6-31*). The optimized structures were saved as mol2 files along with their electrostatic charges.

The crystal structure of *Nicotiana tabacum* PPO was obtained from 1sez (Koch et al., 2004). Prior to use for docking studies, the pdb file was modified to replace the seleniomethionine residues with methionine residues. Also, the atom types of the FAD cofactor were corrected, and the ligand was converted to its oxidized form using Spartan18.

Table 1 - Pre-emergence activity of 4-chloro-2-pentenamides on Palmer amaranth. Data expressed as percent injury

Compounds	Pre-emergence application (g ha^{-1})[1]		
	30	150	300
	Injury (%)[2]		
AGR001	40	90	100
AGR002	20	90	100
AGR003	*nt*[1]	*nt*	100
AGR004	*nt*	*nt*	80
AGR005	*nt*	*nt*	70
AGR006	*nt*	*nt*	100
AGR007	*nt*	*nt*	80
AGR008	*nt*	*nt*	80
AGR009	30	80	85
AGR010	30	30	90
AGR011	0	20	90
AGR012	10	10	0
AGR013	*nt*	*nt*	40
AGR014	*nt*	*nt*	0

[1] n = 3 replicates; *nt*=not tested; [2] Injury rating scale: 0%, no plant phytotoxicity; 100%, plant death.

Table 2 - Post-emergence activity of 4-chloro-2-pentenamides on Palmer amaranth. Data expressed as percent injury

Compounds	Post-emergence application (g ha^{-1})[1]				
	25	50	75	100	250
	Injury (%)[2]				
AGR001	90	95	*nt*	100	*nt*
AGR002	*nt*	30	*nt*	30	50
AGR003	70	100	*nt*	100	100
AGR004	100	100	100	*nt*	*nt*
AGR005	100	90	100	*nt*	*nt*
AGR007	*nt*	*nt*	*nt*	*nt*	80
AGR008	65	90	*nt*	*nt*	95
AGR010	*nt*	*nt*	*nt*	*nt*	50

[1] n = 3 replicates; *nt*=not tested; [2] Injury rating scale: 0%, no plant phytotoxicity; 100%, plant death.

All the herbicides were docked into the catalytic domain of PPO using a Autodock (AutoDock version 4.2, Scripps Institute, San Diego CA, USA) (Goodsell et al., 2021; Morris et al., 2012). Additionally, the guanidino group of arginine 98 (atom id=3782) was designated as important in the interaction between one of the propionate groups (coordinates of this proton are x = -43.390, y = -1.054 and z = 31.750). A grid box was used to delimitate the region of the catalytic domain according to the software. The gridbox dimensions were set to 38Í34Í34 points with a spacing to 0.375. The box was centered on the following coordinates: x = -40, y = -6, and z = 29. PPO was set as a rigid structure. The algorithm was set to generate 100 docking poses and the top clustered was selected as optimal conformation for the docking of each ligand. Interactions between the ligand and the catalytic domain of PPO were identified using the protein–ligand interaction profiler (PLIP) (Salentin et al., 2015).

Prior to docking AGR001 and AGR002, the ligand (OMN or (5-[4-bromo-1-methyl-5-(trifluoromethyl)pyrazol-3-yl]-2-chloro-4-fluoro-benzoic acid)) co-crystalized with PPO in 1sez (Koch et al., 2004) was redocked using Autodock. The ligand's most favored docking pose was similar to the coordinate in the crystal structure (Supplemental Table 1). We also docked all known commercial group 14 herbicides (23 compounds) with Autodock to validate the methodology. All of these inhibitors docked within the same region of the PPO catalytic domain with lower docking energy than AGR001 and AGR002 (Supplemental Table 2).

3. Results and Discussion

The iterative process of Agresense resulted in a family of compounds, AGR001-AGR014 with herbicidal activity described in this paper (Supplemental Table 3). This iterative process is outlined in Figure 1. A database of ~1.2B compounds was screened to create a dynamic library of 20 compounds with diverse molecular structures predicted by Agresense to have herbicidal activity. These compounds were tested in lab assays on Palmer amaranth seedlings to validate their activity, and the results were incorporated in the system to optimize the predictive model. Out of these 20 compounds, one compound outperformed with respect to its herbicidal activity, and this compound served as a structural 'seed' to an additional expanded library of 24 compounds. Additional cycle of lab assays and model optimization resulted in an optimized library of 50 compounds with similar molecular structure. Out of which, 14 compounds (AGR001-AGR014) showed good herbicidal activity in lab assays.

The log*P* values calculated by SwissADME (Daina et al., 2017) are on the higher end of suggested values for biological relevance regarding herbicide uptake, as the "Briggs rule" suggests ideal values are less than 3. Surprisingly, the classifier algorithm predicted these compounds to belong to Herbicide Resistance Action Committee (HRAC) group 14 (inhibitors of PPO), even though classical similarity methods showed extremely low similarity scores to the structure of known group 14 herbicide (Figure 2a). PPO inhibitors registered to date share structural similarities to the substrate, protoporphyrinogen (protogen). In the registered classes of PPO inhibitors, the diphenyl ethers, *n*-phenyl-oxadiazolones, pyraflufen-ethyl and some members of the *n*-phenyl imides and *n*-phenyl-triazolinones have a two-ring structure which mimics one half of protogen. The others, pyraclonil and the rest of the *n*-phenyl imides and *n*-phenyl-triazolinones have three ring structures that still roughly resemble one half to three fourths of a protogen molecule (HRAC). Half of the structures reported in this paper do contain a single cyclic group. The usefulness of PPO inhibitors is evident in extensive research using computational approaches to discover new chemical classes targeting this enzyme (Hao et al., 2017; Wang et al., 2017; Zuo et al., 2016).

3.1 Herbicidal activity

Pre-emergent applications were tested for all 14 potential compounds, post-emergent applications were tested for the top 8 compounds. Pre-emergent activity was investigated in Palmer amaranth, post emergent activity was investigated in rough cocklebur, chinese thorn-apple, black nightshade, mat amaranth, and Palmer amaranth. Despite borderline log*P* values, these compounds were herbicidal. Most tested compounds, other than AGR012 and AGR014 had some pre-emergent activity, with AGR001, AGR002 and AGR009 providing good control (80% or above) at 150 g ha^{-1} (Table 1). Each of the 8 compounds tested post-emergent had good activity, though AGR001, AGR004 and AGR005 were the most active, providing 90% control or above at 25 g ha^{-1} (Table 2). Some of the compounds caused photobleaching, which was consistent with predicted activity as PPO inhibitors. Post-emergent activity of AGR001 in net-house conditions is illustrated in Figure 2b. 7 d after application of 300 g ha^{-1}, at least 85% control was observed for all tested weeds. AGR001 and AGR002 were selected as representative compounds of the structures with herbicidal activity to determine MoA.

3.2 Mode of action studies

PPO inhibitors target the last common enzyme in the synthesis of heme and chlorophyll, a branch point in the tetrapyrrole pathway (Dayan et al., 2020). This causes a buildup of the substrate, protoporphyrinogen, which leaks from the plastids to the cytoplasm and is oxidized into the product of the protein, protoporphyrin IX (proto). Proto is a photodynamic red pigment which generates reactive oxygen species (ROS) upon exposure to light. Subsequently, lipid peroxidation of the cell membranes caused by these ROS disrupts plasma membrane integrity, and ultimately

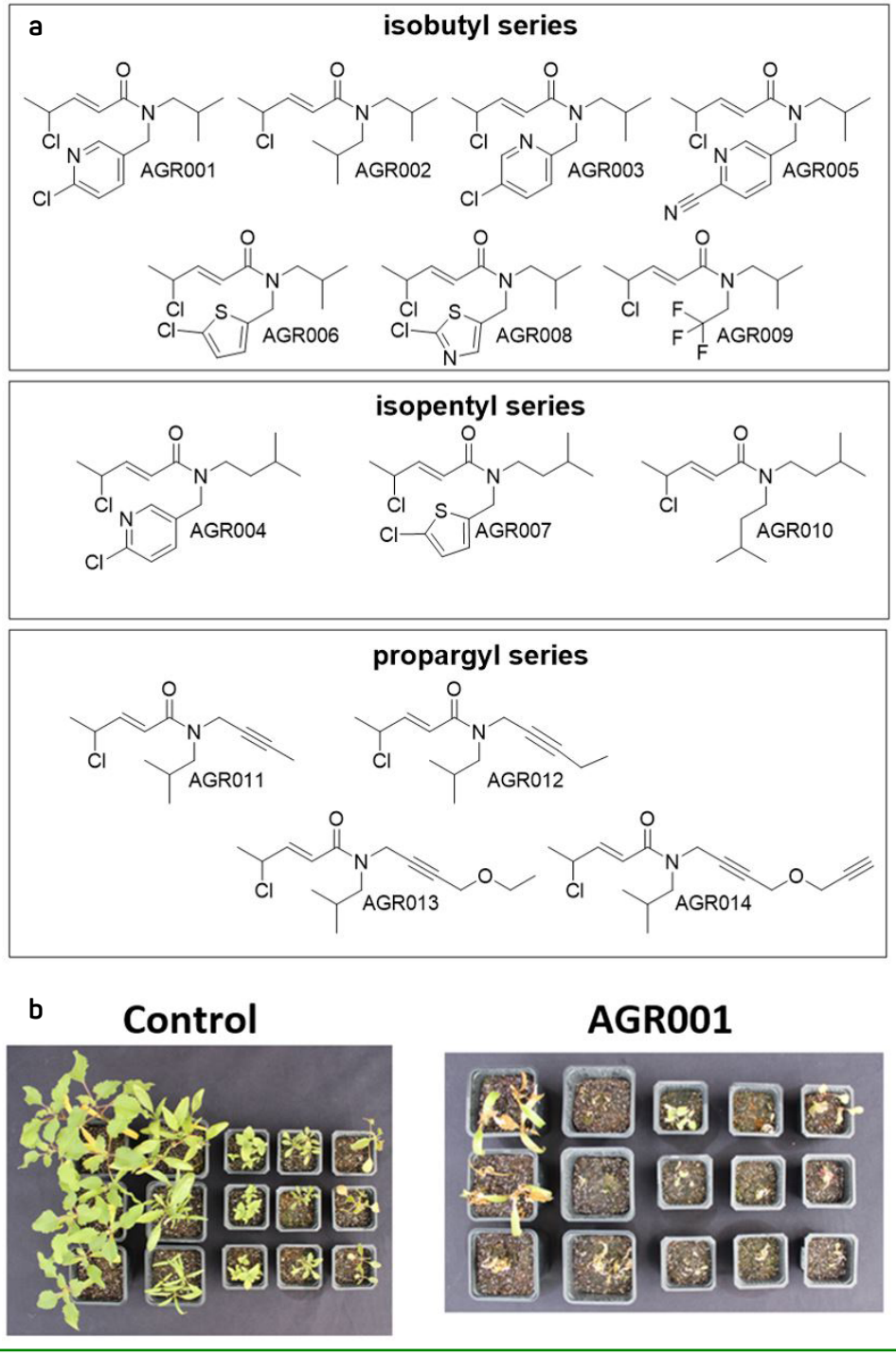

Figure 2 - **a)** Structure of the novel 4-halo-2-pentenamides described in this paper; **b)** Herbicidal activity of AGR001 in post-emergence Net-house assay, 7 days after application of 300 g ha^{-1}. From left to right: rough cocklebur (*Xanthium strumarium*), chinese thorn-apple (*Datura quercifolia*), black nightshade (*Solanum nigrum*), mat amaranth (*Amaranthus blitoides*), Palmer amaranth (*Amaranthus palmeri*).

causes plant death (Dayan et al., 2020). The activity of PPO inhibitors is quantifiable in plant tissue through light-dependent bleaching of tissue, light-dependent electrolyte leakage from membrane disruption, and accumulation of proto after application. Activity can also be observed *in vitro* through an enzyme assay.

Initial electrolyte leakage assays were performed in cucumber cotyledons. Both AGR001 and AGR002 treatments at 100 µM showed the same increase in conductivity due to cell damage after exposure to light as has been reported previously with PPO inhibitors (Figure 3a) (Duke et al., 1991). The second electrolyte

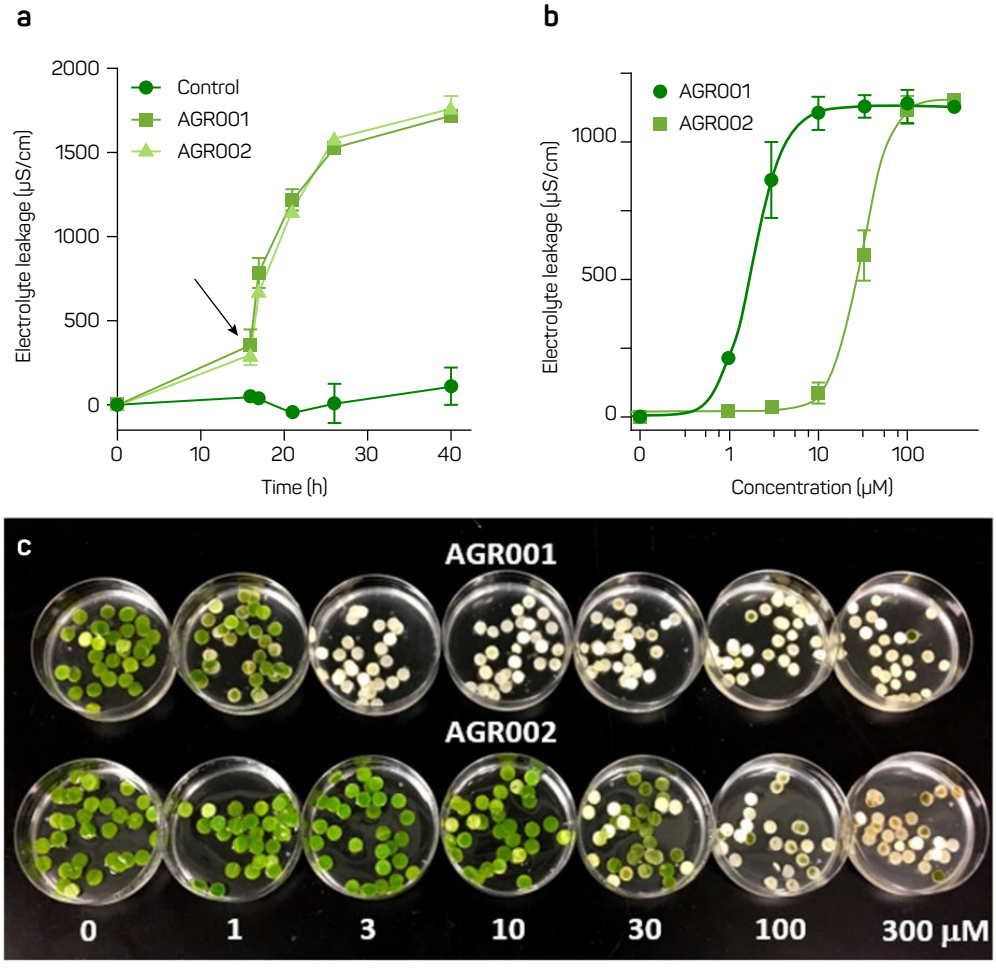

Figure 3 - Electrolyte leakage experiments in cucumber cotyledons. **a)** Electrolyte leakage caused by 100 µg mL^{-1} AGR001 (square) or AGR002 (triangle) over 40 h. Control is shown as circles. The arrow indicates when the plates started exposure to high light intensity (approx. 1400 µmol m^{-2} s^{-1}), n=3 replicates and error bars represent standard deviation; **b)** Dose-response curves with AGR001 (circle) and AGR002 (lsquare) following 15 h dark incubation and 11 h of exposure to high light intensity, n=3 replicates and error bars represent standard deviation; **c)** Bleaching of tissues at the end of the dose-response curve experiments.

leakage assay in cucumber cotyledons was to determine the efficacy of lower doses, showing that AGR001 is approximately sixteen times more active than AGR002, with I_{50} values of 1.8±0.1 µM and 30.0±1.1 µM, respectively (Figure 3b). The bleaching observed in the leaf disks is typical of herbicides inhibiting PPO (Figure 3c).

Additional experiments measuring proto levels in plant tissues exposed to 300 µM of selected compounds were performed. The accumulation of proto in treated tissue and not the control is a characteristic unique to group 14 herbicides, further supporting that these 4-chloro-2-pentenamides target PPO (Figure 4).

A third electrolyte leakage assay was performed on leaf disks from PPO-resistant (Salas et al., 2016) and wildtype Palmer amaranth populations. The PPO-resistant line was not sensitive to either compound (Figure 5b), whereas the susceptible line responded to the treatments with a marked increase in electrolyte leakage over time (Figure 5a).

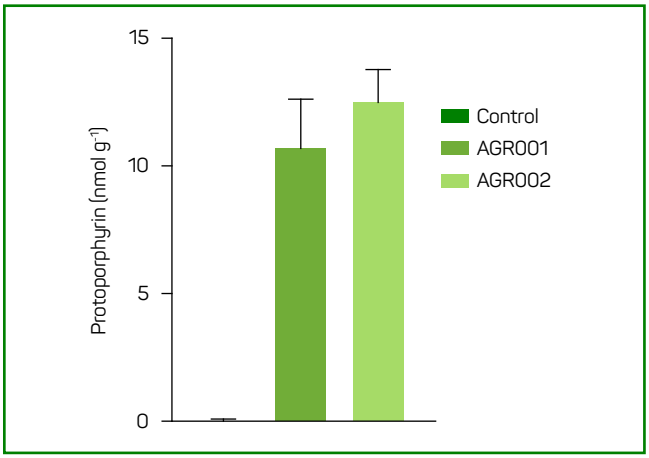

Figure 4 - Accumulation of proto in cucumber cotyledons after 24 h exposure to 300 µM AGR001 (green) or AGR002 (light green) in darkness, relative to DMSO control, n=3 replicates, and error bars represent standard deviation.

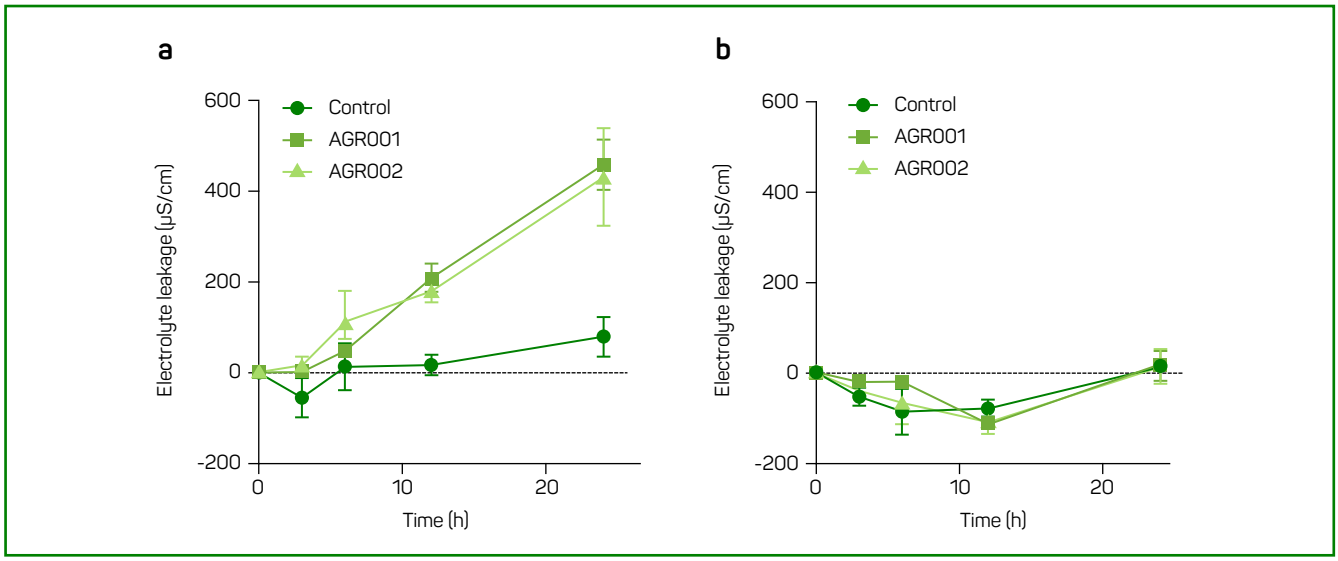

Figure 5 - Electrolyte leakage caused by 10 µM AGR001 (square) and 100 µM AGR002 (triangle) after 15 h dark incubation and subsequent exposure to high light intensity over 24 h on **a)** susceptible and **b)** PPO-resistant Palmer amaranth. Control is shown as circle. n=3 replicates, and error bars represent standard deviation.

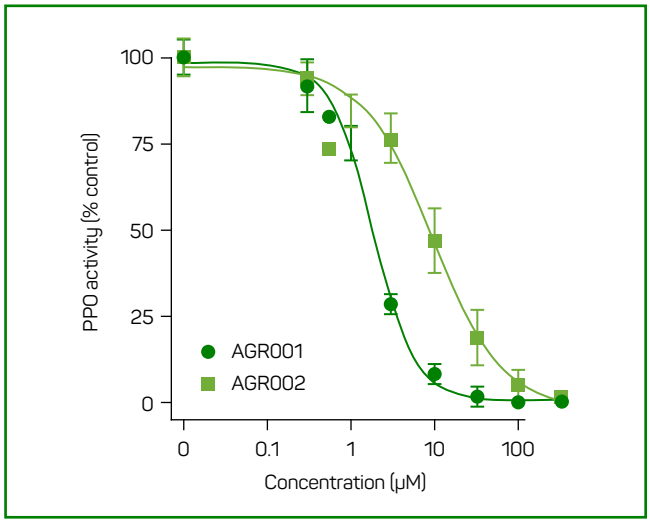

Figure 6 - Inhibition of PPO activity by novel 4-chloro-2-pentenamides in in vitro assays using heterologously expressed enzyme. I50 values for AGR001 (circle) and AGR002 (square) were 1.84±0.11 and 9.42±1.37 µM, respectively. n=3 replicates, and error bars represent standard deviation.

Finally, the MoA of these compounds was confirmed by directly testing on purified PPO enzyme extracted from recombinant wild-type *Amaranthus tuberculatus* PPO2 heterologously expressed in *Escherichia coli* (Figure 6). Dose-response curves were obtained for AGR001 and AGR002 at concentrations ranging from 0.3 to 333 µM. Inhibition of PPO activity by AGR001 and AGR002 was lower than most commercial PPO inhibitors, requiring micromolar concentrations to inhibit 50% of PPO enzyme activity, with I_{50} values of 1.84±0.11 and 9.42±1.37 µM, respectively. Most commercial PPO-inhibiting herbicides have I_{50} values in the submicromolar range (Dayan, Allen, 2000; Dayan et al., 1999). Nonetheless, the *in vitro* activity of AGR001 and AGR002 (Figure 6) paralleled their ability to induce lipid peroxidation and loss of membrane integrity (Figures 3b and c)

The predictive ability of the Agresense artificial intelligence algorithm system for rational identification of the mode of action of novel molecules was confirmed *post facto* following extensive literature searches that identified earlier papers describing the herbicidal activity of related alkenamide compounds (Matsunari et al., 1999a; Matsunari et al., 1999b). The activity of these compounds was light-dependent and was later associated with inhibition of PPO (Hiraki et al., 2002; Matsunari et al., 2002).

3.3 Docking study

Docking studies were performed to further understand the interaction between AGR001 and AGR002 with the catalytic domain of PPO. The published binding energy of protogen and proto are -10.6 and -7.3 kcal mol^{-1}, respectively (Barker et al., 2020). The average docking energies for AGR001 and AGR002 were -4.7 and -3.1 kcal mol^{-1}, respectively. These values are lower than the binding energies of other common PPO inhibitors, which range from -8.8 to -5.3 kcal mol^{-1}, indicating a less effective binding to the active site which is reflected in the higher I_{50} values reported above (Supplemental Table 2). AGR001 and AGR002 are smaller and structurally different from all commercial PPO-inhibiting herbicides. 4-Chloro-2-pentenamides have very flexible side chains and can hold several different conformations in the active site (Figure 7a and Supplemental Figure 2), whereas most PPO inhibitors are more rigid multicyclic molecules that occupy a more limited number of poses and are stabilized

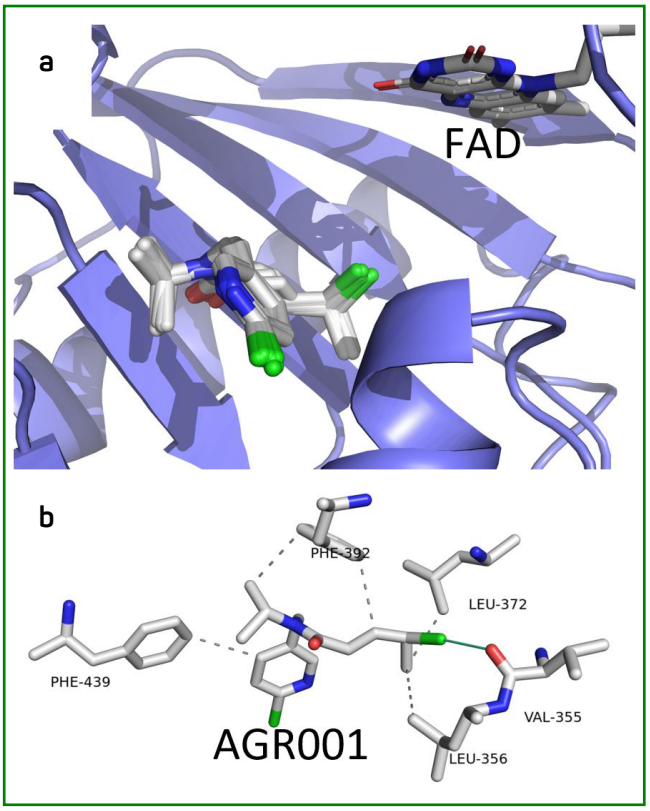

Figure 7 - **a)** Representative docking poses of AGR001 with lowest energy in PPO binding domain from Autodock analysis (protein is in light blue and FAD is positioned on top of catalytic domain). A total of 18 molecules docked in this position, with an average calculated docking energy of -4.98 kcal mol^{-1}. **b)** Most favored docking pose of AGR001 and its Interaction with key residues in the binding pocket of PPO obtained using the protein–ligand interaction profiler (PLIP) (Salentin et al., 2015) after 100 Autodock iterations. Gray dotted line = hydrophobic interaction; green solid line = halogen interaction. Refer to Supplemental Table 2 for total number of poses in each group and their respective docking energies for both AGR001 and AGR002, Supplemental Figure 2 for illustrations of the other docking poses in PPO and Supplemental Figure 3 for illustrations of the protein ligand interactions for both AGR001 and AGR002.

by interactions with highly conserved residues (e.g., Arg98, Phe353 and Leu356) known to interact with the substrate in the catalytic domain (Figure 7b and Supplemental Figure 3). Most of the interactions involved hydrophobic interactions between the ligand and the surrounding residues. A few poses also involved hydrogen bonding. This ability of 4-chloro-2-pentenamides to assume different poses within the catalytic domain indicates an increase in entropic energy compared to other PPO inhibitors and may account for the low binding energies of this chemical class.

4. Conclusions

The discovery of new herbicides is critical to sustain crop productivity around the globe. Agrematch has introduced a transformative approach to explore chemical spaces for bioactive compound discovery. Their AI system utilizes large data sets and advanced machines and DL algorithms to identify and then biologically validate leads with new modes of action. This innovative approach vastly expands the reach into the chemical space that will lead to the discovery of much needed new products. The 4-chloro-2-pentenamides identified as putative PPO inhibitors by the Agresense AI algorithm have both pre- and post-emergent herbicidal activity on multiple weeds. Compounds AGR001 and AGR002 were the most potent with respect to post-emergence application, demonstrating almost complete Palmer amaranth control at 150 g ha^{-1} rate. Compounds AGR001, AGR004 and AGR005 were the most potent with respect to pre-emergence application, demonstrating almost complete Palmer amaranth control at 25 g ha^{-1}. While the effectiveness of compound AGR001 was observed to be significant against a variety of dicot weeds, its performance against monocot weeds was comparatively lower (data not shown). The findings of this study indicate that the compounds exhibit greater post-emergence activity than pre-emergence activity. However, it is important to acknowledge that the choice of soil in pre-emergence assays can significantly influence the efficacy of herbicides. Despite the lack of structural similarity with known PPO inhibitors, these compounds indeed acted by inhibiting PPO, causing the expected light-dependent loss of membrane integrity, photobleaching, accumulation of proto and inhibition of PPO. These alkenamides are not as potent as current commercial group 14 herbicides, but one should keep in mind that these structures are lead compounds that require further structural optimization and formulation to improve their efficacy. While some weeds have evolved resistance to certain PPO-inhibiting chemistry, group 14 herbicides remain an important group of chemicals to manage weeds (Barker et al., 2023; Dayan et al., 2018; Dayan, Duke, 1997), and many major agrochemical companies are developing new molecules with this mode of action (Mattison et al., 2023; Porri et al., 2023). Unfortunately, these 4-chloro-2-pentenamides do not overcome resistance imparted by a Gly210 deletion. The Agresense algorithm continues to identify novel chemical spaces with potentially new MoAs.

5. Author's contributions

All authors read and agreed to the published version of the manuscript.

ALB, YG, ES, NS, YP, IS, and FED: conceptualization of the manuscript and development of the methodology. ALB, YG, ES, NS, YP, IS, and FED: Data collection and curation. ALB, YG, ES, NS, YP, IS, and FED: data analysis and interpretation. ALB and FED: writing the original draft of the manuscript ALB, YP, IS, and FED: writing, review and editing

6. Funding

This research was supported in part by Agrematch Ltd and the USDA National Institute of Food and Agriculture, Hatch Project 1016591, COL00785.

References

Barker AL, Barnes H, Dayan FE. Conformation of the intermediates in the reaction catalyzed by protoporphyrinogen oxidase: an *in silico* analysis. Internat J Mol Sci. 2020;21(24):1-12. Available from: https://doi.org/10.3390/ijms21249495

Barker AL, Pawlak J, Duke SO, Beffa R, Tranel PJ, Wuerffel J et al. Discovery, mode of action, resistance mechanisms, and plan of action for sustainable use of Group 14 herbicides. Weed Sci. 2023;71(3):173-88. Available from: https://doi.org/10.1017/wsc.2023.15

Cooper J, Dobson H. The benefits of pesticides to mankind and the environment. Crop Protect. 2007;26:1337-48. Available from: https://doi.org/10.1016/j.cropro.2007.03.022

Daina A, Michielin O, Zoete V. SwissADME: a free web tool to evaluate pharmacokinetics, drug-likeness and medicinal chemistry friendliness of small molecules. Sci Rep. 2017;7(1):1-13. Available from: https://doi.org/10.1038/srep42717

Dayan FE. Current status and future prospects in herbicide discovery. Plants. 2019;8(9):1-18. Available from: https://doi.org/10.3390/plants8090341

Dayan FE, Allen SN. Predicting the activity of the natural phytotoxic diphenyl ether cyperine using Comparative Molecular Field Analysis. Pest Manage Sci. 2000;56(8):717-22. Available from: https://doi.org/10.1002/1526-4998(200008)56:8<717::AID-PS183>3.0.CO;2-0

Dayan FE, Barker A, Takano H, Bough R, Ortiz M, Duke SO. Herbicide mechanisms of action and resistance. In: Moo-Young M, editor. Comprehensive biotechnology vol. 3. Amsterdam: Elsevier; 2020. p. 36-48.

Dayan FE, Barker A, Tranel PJ. Origins and structure of chloroplastic and mitochondrial plant protoporphyrinogen oxidases: implications for the evolution of herbicide resistance. Pest Manage Sci. 2018;74(10):2226-34. Available from: https://doi.org/10.1002/ps.4744

Dayan FE, Daga PR, Duke SO, Lee RM, Tranel PJ, Doerksen RJ. Biochemical and structural consequences of a glycine deletion in the α-8 helix of protoporphyrinogen oxidase. Biochim Biophys Acta. 2010;1804(7):1548-56. Available from: https://doi.org/10.1016/j.bbapap.2010.04.004

Dayan FE, Duke SO. Phytotoxicity of protoporphyrinogen oxidase inhibitors: phenomenology, mode of action and mechanisms of resistance. In: Roe RM, Burton JD, Kuhr RJ, editors. Herbicide activity: toxicology, biochemistry and molecular biology. Amsterdam: IOS; 1997. p. 11-35.

Dayan FE, Duke SO. Protoporphyrinogen oxidase-inhibiting herbicides. In: Krieger R, editor. Haye's handbook of pesticide toxicology. 3rd. ed. San Diego: Academic; 2010. p. 1733-51.

Dayan FE, Owens DK, Corniani N, Silva FML, Watson SB, Howell JL et al. Biochemical markers and enzyme assays for herbicide mode of action and resistance studies. Weed Sci. 2015;63(sp1):23-63. Available from: https://doi.org/dx.doi.org/10.1614/WS-D-13-00063.1

Dayan FE, Reddy KN, Duke SO. Structure-activity relationships of diphenyl ethers and other oxygen-bridged protoporphyrinogen oxidase inhibitors. In: Böger P, Wakabayashi K editors. Peroxidizing herbicides. Berlin: Springer-Verlag; 1999. p. 141-61.

Dayan FE, Watson SB. Plant cell membrane as a marker for light-dependent and light-independent herbicide mechanisms of action. Pestic Biochem Physiol. 2011;101(3):182-90. Available from: https://doi.org/10.1016/j.pestbp.2011.09.004

Duke SO, Lydon J, Becerril JM, Sherman TD, Lehnen LP, Matsumoto H. Protoporphyrinogen oxidase-inhibiting herbicides. Weed Sci. 1991;39(3):465-73. Available from: https://doi.org/10.1017/S0043174500073239

Fennimore SA, Cutulle M. Robotic weeders can improve weed control options for specialty crops. Pest Manage Sci. 2019;75(7):1767-74. Available from: https://doi.org/10.1002/ps.5337

Gaines TA, Duke SO, Morran S, Rigon CAG, Tranel PJ, Küpper A et al. Mechanisms of evolved herbicide resistance. J Biol Chem. 2020;295(3):10307-30. Available from: https://doi.org/10.1074/jbc.REV120.013572

Goodsell DS, Sanner MF, Olson AJ, Forli S. The AutoDock suite at 30. Protein Sci. 2021;30(1):31-43. Available from: https://doi.org/10.1002/pro.3934

Hao G-F, Zuo Y, Yang S-G, Chen Q, Zhang Y, Yin C-Y et al. Computational discovery of potent and bioselective protoporphyrinogen IX oxidase inhibitor via fragment deconstruction analysis. J Agric Food Chem. 2017;65(28):5581-8. Available from: https://doi.org/10.1021/acs.jafc.7b01557

Heap I. The international survey of herbicide resistant weeds. Weedscience. 2023[access May 2023]. www.weedscience.org

Hiraki M, Matsunari K, Fujita T, Wakabayashi K. Mode of action of herbicidal *N*-benzyl-4-chloro-*N*-isobutyl-2-pentenamides. J Pestic Sci. 2002;27(3):272-4. Available from: https://doi.org/10.1584/jpestics.27.272

Jacobs NJ, Jacobs JM. Assay for enzymatic protoporphyrinogen oxidation, a late step in heme synthesis. Enzyme. 1982;28:206-19. Available from: https://doi.org/10.1159/000459103

Kim S, Chen J, Cheng T, Gindulyte A, He J, He S et al. PubChem in 2021: new data content and improved web interfaces. Nucleic Acids Res. 2021;49(D1):D1388-95. Available from: https://doi.org/10.1093/nar/gkaa971

Koch M, Breithaupt C, Kiefersauer R, Freigang J, Huber R, Messerschmidt A. Crystal structure of protoporphyrinogen IX oxidase: a key enzyme in haem and chlorophyll biosynthesis. Embo J. 2004;23:1720-8. Available from: https://doi.org/10.1038/sj.emboj.7600189

Matsunari K, Shimizu T, Yoshida F, Fujita T. Mechanism of the phytotoxic action of herbicidal *N*-isobutyl-*N*-(4-substituted benzyl)-4-halo-2-pentenamides. J Pestic Sci. 2002;27(1):9-16. Available from: https://doi.org/10.1584/jpestics.27.9

Matsunari K, Sugiyama H, Sadohara H, Motojima K. Synthesis and herbicidal activity of *N*-alkyl-*N*-(substituted benzyl)-4-ha-

lo-2-alkenamides. J Pestic Sci. 1999a;24(1):1-6. Available from: https://doi.org/10.1584/jpestics.24.1

Matsunari K, Yoshida F, Nakamura Y, Fujita T. Quantitative structure-activity relationships of herbicidal *N*-alkyl-*N*-(4-substituted benzyl)-4-chloro-2-pentenamides against *Echinochloa oryzicola*. J Pestic Sci. 1999b;24(1):7-12. Available from: https://doi.org/10.1584/jpestics.24.7

Mattison RL, Beffa R, Bojack G, Bollenbach-Wahl B, Dörnbrack C, Dorn N et al. Design, synthesis and screening of herbicidal activity for new phenyl pyrazole-based protoporphyrinogen oxidase-inhibitors (PPO) overcoming resistance issues. Pest Manage Sci. 2023;79(6):2264-80. Available from: https://doi.org/10.1002/ps.7425

Morris GM, Goodsell DS, Pique ME, Lindstrom W, Huey R, Forli S et al. AutoDock version 4.2 automated docking of flexible ligands to flexible receptors: user guide. AutoDock. 2012. Available from: https://doi.org/https://autodock.scripps.edu/wp-content/uploads/sites/56/2021/10/AutoDock4.2.6_UserGuide.pdf

Moulin M, Smith AG. A robust method for determination of chlorophyll intermediates by tandem mass spectrometry. In: Allen JF, Gantt E, Golbeck JH, Osmond B, editors. Photosynthesis energy from the sun: 14th international congress on photosynthesis. Dordrecht: Springer; 2008. p. 1215-22.

Muller C, Rabal O, Diaz Gonzalez C. Artificial intelligence, machine learning, and deep learning in real-life drug design cases. In: Heifetz A, editor. Artificial intelligence in drug design. New York: Springer; 2022. p. 383-407.

Patzoldt WL, Hager AG, McCormick JS, Tranel PJ. A codon deletion confers resistance to herbicides inhibiting protoporphyrinogen oxidase. Proc Natl Acad Sci USA. 2006;103(33):12329-34. Available from: https://doi.org/10.1073/pnas.0603137103

Peters B, Strek HJ. Herbicide discovery in light of rapidly spreading resistance and ever-increasing regulatory hurdles. Pest Manage Sci. 2018;74(10):2211-5. Available from: https://doi.org/10.1002/ps.4768

Pimentel D, Zuniga R, Morrison D. Update on the environmental and economic costs associated with alien-invasive species in the United States. Ecol Econ. 2005;52(3):273-88. Available from: https://doi.org/10.1016/j.ecolecon.2004.10.002

Porri A, Betz M, Seebruck K, Knapp M, Johnen P, Witschel M et al. Inhibition profile of trifludimoxazin towards PPO2 target site mutations. Pest Manage Sci. 2023;79(2):507-19. Available from: https://doi.org/10.1002/ps.7216

Ritz C, Baty F, Streibig JC, Gerhard D. Dose-response analysis using R. PLoS ONE. 2015;10(12):1-13. Available from: https://doi.org/10.1371/journal.pone.0146021

Salas-Perez RA, Burgos NR, Rangani G, Singh S, Paulo Refatti J, Piveta L et al. Frequency of Gly-210 deletion mutation among protoporphyrinogen oxidase inhibitor-resistant Palmer amaranth (*Amaranthus palmeri*) populations. Weed Sci. 2018;65(6):718-31. Available from: https://doi.org/10.1017/wsc.2017.41

Salas RA, Burgos NR, Tranel P, Singh S, Glasgow L, Scott RC et al. Resistance to PPO-inhibiting herbicide in Palmer amaranth from Arkansas, USA. Pest Manage Sci. 2016;72(5):864-9. Available from: https://doi.org/10.1002/ps.4241

Salentin S, Schreiber S, Haupt VJ, Adasme MF, Schroeder M. PLIP: fully automated protein–ligand interaction profiler. Nucleic Acids Res. 2015;43(W1):W443-7. Available from: https://doi.org/10.1093/nar/gkv315

Soltani N, Dille JA, Burke IC, Everman WJ, VanGessel MJ, Davis VM, et al. Potential corn yield losses from weeds in North America. Weed Technol. 2016;30(4):979-84, 6. Available from: https://doi.org/10.1614/WT-D-16-00046.1

von Lilienfeld OA, Burke K. Retrospective on a decade of machine learning for chemical discovery. Nat Commun. 2020;11(1):1-4. Available from: https://doi.org/10.1038/s41467-020-18556-9

Wang D-W, Li Q, Wen K, Ismail I, Liu DD, Niu CW et al. Synthesis and herbicidal activity of pyrido[2,3-d]pyrimidine-2,4-dione–benzoxazinone hybrids as protoporphyrinogen oxidase inhibitors. J Agric Food Chem. 2017;65(26):5278-86. Available from: https://doi.org/10.1021/acs.jafc.7b01990

Westwood JH, Charudattan R, Duke SO, Fennimore SA, Marrone P, Slaughter DC et al. Weed management in 2050: perspectives on the future of weed science. Weed Sci. 2018;66(3):275-85. Available from: https://doi.org/10.1017/wsc.2017.78

Zuo Y, Wu Q, Su SW, Niu CW, Xi Z, Yang GF. Synthesis, herbicidal activity, and QSAR of novel *N*-benzothiazolyl-pyrimidine-2,4-diones as protoporphyrinogen oxidase inhibitors. J Agric Food Chem. 2016;64(3):552-62. Available from: https://doi.org/10.1021/acs.jafc.5b05378